AZIMUTH BEAM PATTERN SYNTHESIS FOR AIRBORNE SAR SYSTEM OPTIMIZATION

S. H. Lim and J. H. Han

Department of Electrical Engineering
Korea Advanced Institute of Science and Technology (KAIST)
335 Gwahangno, Yuseong-Gu, Daejeon 305-701, Korea

S. Y. Kim

Image Information PEO
Agency for Defense Development (ADD)
Yuseong-gu, Daejeon, Korea

N. H. Myung

Department of Electrical Engineering
Korea Advanced Institute of Science and Technology (KAIST)
335 Gwahangno, Yuseong-Gu, Daejeon 305-701, Korea

Abstract—The limitation of the pulse repetition frequency (PRF) of an airborne synthetic aperture radar (SAR) system is not a serious problem to obtain high azimuth resolution and wide swath imaging compared with a spaceborne SAR system. Hence, continuous high azimuth resolution imagery over a wide area can be obtained using an antenna having a wide beamwidth. Since a small antenna with a large beamwidth has very low gain, which results in difficulty in detection; the azimuth beam pattern optimization of a large active phased array antenna is needed for airborne SAR system optimization. To improve the airborne SAR system performance, such as the noise-equivalent sigma zero ($NE\sigma_0$), the azimuth resolution, the radiometric accuracy (RA), and the azimuth ambiguity ratio (AAR), we present an optimal azimuth beam pattern mask template and suggest an azimuth beam pattern satisfying the mask template using the particle swarm optimization (PSO). The mode having the proposed beam pattern guarantees continuous and high resolution images, simultaneously.

Using a point target simulation, the advantages of the mode are shown compared to strip-map and spotlight modes.

1. INTRODUCTION

Synthetic aperture radar (SAR) based on doppler signal synthesizing in the azimuth direction is introduced to obtain high azimuth resolution image [1–3]. The basic operating modes of the SAR system can be divided into three modes; strip-map mode, spotlight mode, and wide-scan mode. The strip-map mode can obtain continuous images and guarantees a moderate resolution, and the spotlight mode is used for obtaining high resolution image of limited area using a mechanical or electrical beam steering. The spotlight mode, however, has the disadvantages of narrow swath width and discontinuous images. The wide-scan mode has wide swath width and sparse azimuth resolution. Compared to other modes, this mode has difficulty when the received signals are processed to obtain images.

All three modes use the array antenna having a single phase front, which has a narrow azimuth beamwidth resulting in a small observation area in azimuth direction. This paper suggests an array antenna having an optimal azimuth beam pattern for obtaining wide area information, as shown in Figure 1. Using this method, a continuous image, which is the advantage of the strip-map mode, and a high resolution image, which is the advantage of the spotlight mode, can be obtained simultaneously.

In this paper, we suggest an azimuth beam pattern mask template for a continuous and high resolution image in an airborne SAR system and present an azimuth beam pattern satisfying the mask
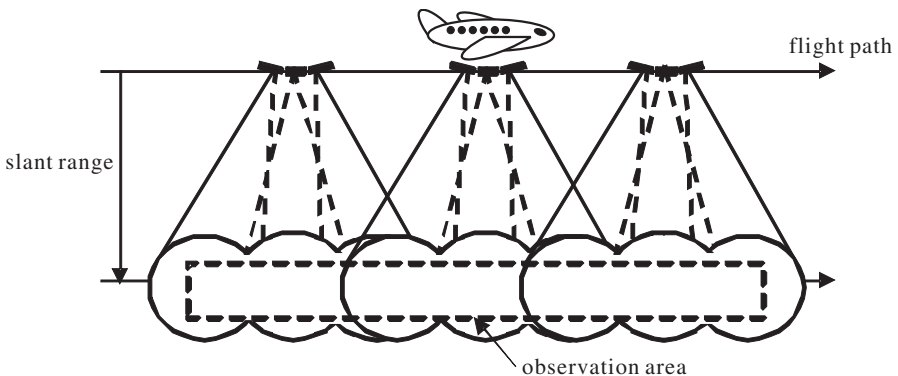

Figure 1. Proposed optimal azimuth beam pattern mode.

using the particle swarm optimization (PSO) [4–13]. Section 2 explains the relation between the SAR system parameters and provides the difference between the spaceborne SAR and the airborne SAR system. Section 3 suggests the beam pattern mask template for the optimization of an airborne SAR system and presents the beam pattern satisfying the mask using the PSO. Section 4 analyzes the performance of the proposed method and verifies the benefits compared to the strip-map mode and the spotlight mode. In Section 5, we present our conclusions.

2. SAR SYSTEM ANALYSIS

Table 1. Required parameters.

Parameters	Symbol
Swath width	W_g
Azimuth resolution	ρ_a
Range resolution	ρ_r

Table 2. Geometric and systemic parameters.

Parameters	Symbol
Platform velocity	v_p
Platform altitude	h_p
Center frequency	f_0
Noise equivalent sigma zero	$NE\sigma_0$
Transmit power	P_t
Antenna range width	W_a
Antenna range beamwidth	θ_r
Antenna azimuth length	L_a
Antenna azimuth beamwidth	θ_a
Chirp pulse width	τ_{chirp}
Pulse repetition frequency	PRF
Target exposure time	t_a
Doppler bandwidth	Δf_d
Chirp pulse band width	ΔBW_{chirp}

Table 1 shows the required parameters such as swath width (W_g), azimuth resolution (ρ_a), and range resolution (ρ_r), which are the pointers of the SAR system performance. To satisfy the required parameters, the geometric and systematic parameters shown in Table 2 must be considered carefully because the parameters affect the system performance with a complex relation between them as illustrated in Figure 2.

To obtain high azimuth resolution, the antenna azimuth beamwidth has to be increased to increase the target exposure time. However, the increasing the target exposure time needs the high PRF which results in the narrow swath width. Therefore, the system constraints must be adjusted properly when broadening the azimuth beamwidth. The trade-off between the azimuth resolution and the swath width in airborne SAR system is different from the one of the spaceborne SAR system and this is explained below.

The azimuth resolution and the swath width of a SAR system can be expressed as (1) and (2), where c denotes the speed of light and θ_i is the incident angle in the range direction. The two equations can be
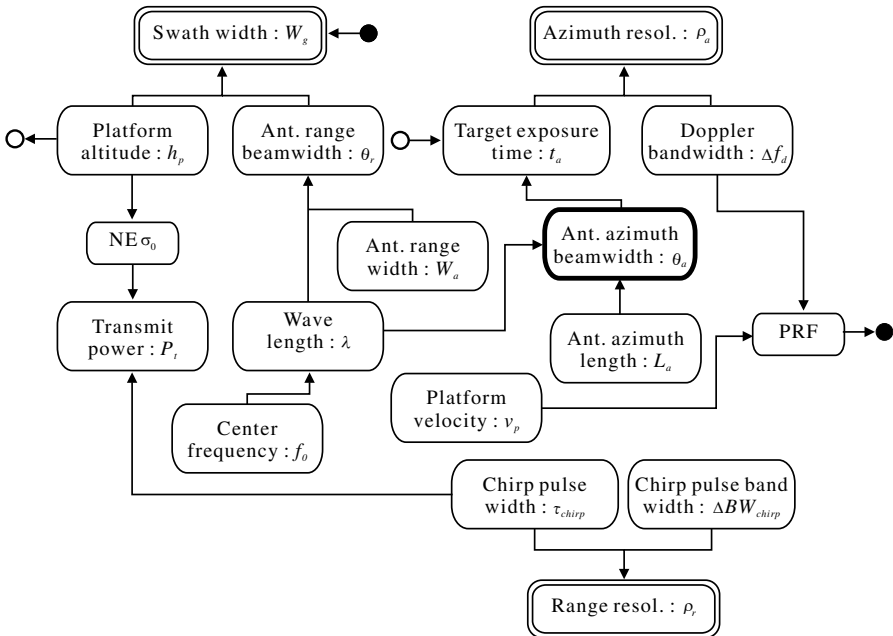

Figure 2. Relation between the SAR system parameters.

unified as (3) in terms of the PRF.

$$\rho_a \approx \frac{L_a}{2} \approx \frac{v_p}{\Delta f_d} \geq \frac{v_p}{PRF} \tag{1}$$

$$W_g \leq \frac{c}{2 \cdot PRF \cdot \sin(\theta_i)} \tag{2}$$

$$\frac{v_p}{\rho_a} < PRF < \frac{c}{2 \cdot W_g \cdot \sin(\theta_i)} \tag{3}$$

Because the platform velocity of the airborne SAR system is slower than the one of the spaceborne SAR system and the altitude of the airborne SAR system is also lower than the one of the spaceborne SAR system, the airborne SAR system has a wide margin in terms of PRF. Thus, high resolution and wide swath imaging can be obtained in the airborne SAR system using high PRF, which results from the large azimuth beamwidth. If we use a small antenna to obtain wide beamwidth, the received signals are not detectable due to the small antenna gain. It is, therefore, important to optimize the azimuth beam pattern using the individual element antenna amplitude and phase control of a large active phased array antenna. The following section explains algorithms how to make the optimum azimuth beam pattern for the airborne SAR system performance optimization.

3. AZIMUTH BEAM PATTERN MASK TEMPLATE AND BEAM PATTERN THEREOF

The optimization of an airborne SAR system is to increase the range resolution, the azimuth resolution, the swath width, and the radiometric accuracy (RA), and to decrease the noise-equivalent sigma zero ($NE\sigma_0$), the range ambiguity ratio (RAR), and the azimuth ambiguity ratio (AAR). The range resolution is determined by the chirp pulse bandwidth and the RA, the $NE\sigma_0$, the RAR for the range direction depends on the range beam pattern of the antenna, as explained in detail in [10, 11]. In this paper, we focus on the optimization of the azimuth beam pattern for increasing the azimuth resolution and the RA in the azimuth direction and decreasing the $NE\sigma_0$ and the AAR. Figure 3 shows how the azimuth beam pattern influences the parameters mentioned above. The $NE\sigma_0$ is affected by the antenna gain, and high gain guarantees low $NE\sigma_0$. The azimuth resolution is determined by the beamwidth of the main lobe, and the wider beamwidth, the finer the resolution. The RA is calculated by the flatness of the main lobe, and the flatter the main lobe, the better the RA. Finally, the AAR is controlled by the shape of the side lobe.
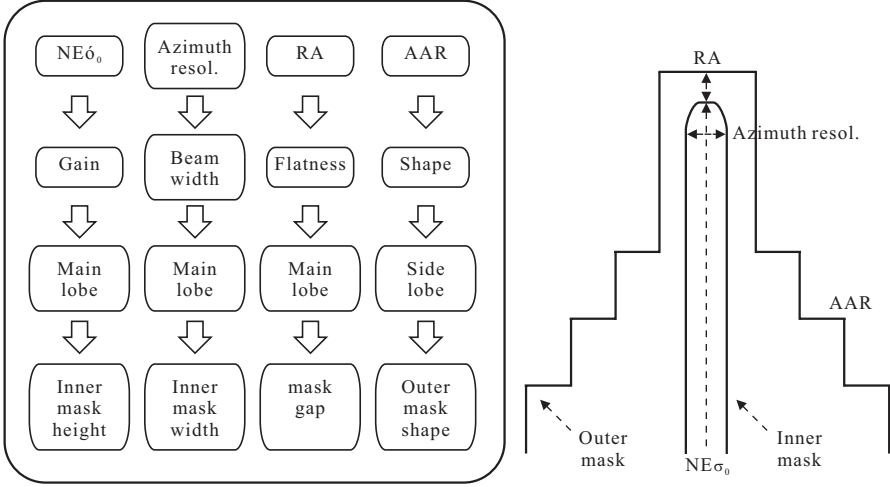
Figure 3. Performance effects due to azimuth antenna pattern.

Making the shape like a stairway is one of the best methods to obtain low AAR and high antenna gain simultaneously.

To create an optimum azimuth beam pattern mask template, we performed the following tasks. First, we determined the gain of the main lobe based on the required minimum $NE\sigma_0$ as (4), where R is the slant range, k is the Boltzmann constant, T_0 is the absolute temperature, NF is the system noise figure, L_{tot} is the total loss of the SAR system, G_t is the transmit antenna gain, and G_r is the receive antenna gain. When an identical antenna was used for transmitting and receiving, the minimum antenna gain was calculated as (5) based on the required minimum $NE\sigma_0$.

$$NE\sigma_0 = \frac{4 \cdot (4\pi)^3 \cdot R^3 \cdot v_p \cdot \sin(\theta_i) \cdot k \cdot T_0 \cdot NF \cdot \Delta BW_{chirp} \cdot L_{tot}}{\lambda^3 \cdot c \cdot G_t \cdot G_r \cdot \tau_{chirp} \cdot P_t \cdot PRF} \quad (4)$$

$$G_{t,r} = \sqrt{\frac{4 \cdot (4\pi)^3 \cdot R^3 \cdot v_p \cdot \sin(\theta_i) \cdot k \cdot T_0 \cdot NF \cdot \Delta BW_{chirp} \cdot L_{tot}}{\lambda^3 \cdot c \cdot NE\sigma_0 \cdot \tau_{chirp} \cdot P_t \cdot PRF}} \quad (5)$$

After finding the antenna gain, the main lobe beamwidth, which decides the azimuth resolution, is needed to be determined. The relation between the azimuth resolution and the main lobe beamwidth at the reference level of 3 dB is given in (6). Through the same resolution in both the azimuth and range direction, the obtained 2-dimensional image can be viewed without distortion.

$$\theta_a \approx \frac{\lambda}{2 \cdot \rho_a} = \frac{\lambda}{2 \cdot \rho_r} \quad (6)$$

Then, the flatness of the main lobe has to be increased for obtaining high RA. To satisfy the condition, the gap between the inner and the outer mask of the main lobe should be lower than 0.5 dB. Finally, the AAR can be computed by (7), and the shape of the side lobe should be like stairway to achieve low AAR of -20 dB.

$$AAR = \frac{\sum_{m=-\infty, m\neq 0}^{m=\infty} \int_{-B_p/2}^{B_p/2} G^2(f + m \cdot PRF)df}{\int_{-B_p/2}^{B_p/2} G^2(f)df} \tag{7}$$

The suggested optimum azimuth beam pattern mask template provides the optimum azimuth resolution with sufficient $NE\sigma_0$, RA, and AAR for an airborne SAR system. The example parameters are listed in Table 3, and the mask template based on the parameters are shown in Figure 4.

The azimuth beam pattern satisfying the proposed mask template can be found using the PSO [4–13]. It is especially important to select the initial values for searching for the optimum solution. To increase the flatness of the main lobe, the window function can be used when each element antenna's amplitude is decided, and the Kaiser window is one of the best methods for a low integrated sidelobe ratio (ISLR) [14]. We allocated the amplitude and the phase of each element antenna of the array as initial values using the Kaiser window. The fitness function can be used to evaluate the suitability of the particles in the PSO simulation as in (8).

$$\text{Fitness function} = w_m \sum_\theta (P_{md} - P_\theta) + w_s \sum_\theta (P_{sd} - P_\theta), \tag{8}$$

Table 3. Airborne SAR system parameters for optimum mask template.

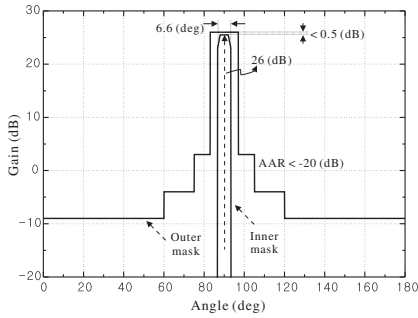| Airborne SAR system parameters			
f_0	9.4 (GHz)	ΔBW_{chirp}	1 (GHz)
v_p	250 (m/s)	L_{tot}	2.9 (dB)
h_p	10 (km)	τ_{chirp}	10 (μs)
θ_i	55 (deg)	$NE\sigma_0$	-20 (dB)
k	1.38e-23	P_t	0.5 (kW)
T_0	290 (K)	PRF	3.1 (kHz)
NF	3.5 (dB)	L_a	1 (m)
Element ant. number	44	Element ant. gap	0.7 λ (m)

Figure 4. Optimum azimuth beam pattern mask template.
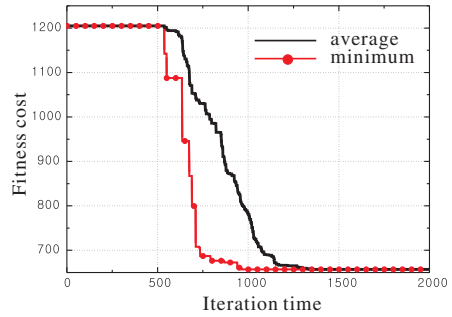

Figure 5. Fitness function of the PSO.

Table 4. PSO parameters for an optimum beam pattern satisfying the mask.

PSO simulation parameters	
Number of particles	20
Iteration number	2000
Initial amplitude distribution	Kaiser window
Initial phase distribution	Kaiser window
Gain control step	0.5 (dB)
Gain control range	$0 \sim -30$ (dB)
Phase control step	5.625 (deg)
Phase control range	$-180 \sim 180$ (deg)

where the w_m and w_s represent the weighings of the main and side lobes and the P_{md} and P_{ms} are the desired main and side lobe patterns based on the suggested mask template. The P_θ is the beam pattern, which is the result using the PSO, and the result having the minimum fitness function becomes the solution.

We assumed that the active phased array antenna has 44 T/R modules in the azimuth direction, with each module having a 6 bit digitally controlled attenuator and a 6 bit digitally controlled phase shifter. Table 4 lists the parameters used in the PSO simulation. Figure 5 shows the average and minimum fitness functions of the PSO with 2000 iteration, and Figure 6 shows the amplitude and the phase distributions of the array antenna as a final solution.

The beam pattern having the mentioned distributions satisfied the suggested optimum beam pattern mask template as shown in Figure 7.
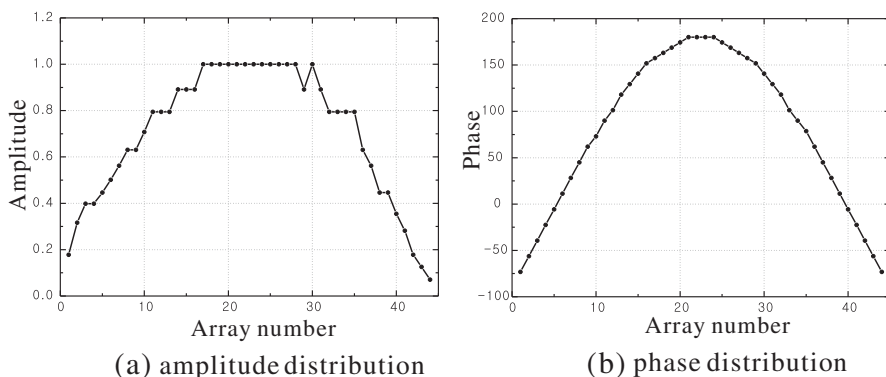
(a) amplitude distribution   (b) phase distribution

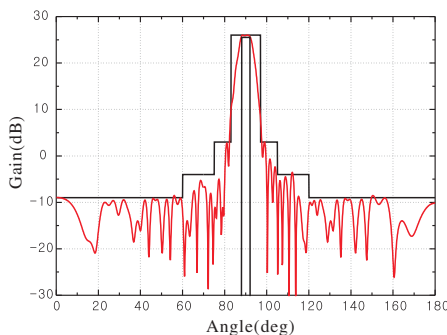**Figure 6.** Amplitude and phase distribution of the array antenna.

Figure 7. The final azimuth beam pattern using the PSO.

The antenna gain of the main lobe is higher than the minimum level in the inner mask. The flatness is 0.11 dB which is much lower than the minimum reference value of 0.5 dB for increasing the RA. The side lobe also satisfied the template with few errors for decreasing the AAR.

In the following section, we carry out the point target simulation to verify the performance of the mode having the beam pattern and show the advantages compared to the strip-map mode and the spotlight mode.

4. IMAGE QUALITY ANALYSIS

Figure 8 shows the flow chart of the SAR system simulation. First, the raw data is generated based on the system parameters listed in Tables 1 and 2. The basic modes such as the strip-map, spotlight, and the wide-scan modes use a sinc-like beam pattern having a narrow
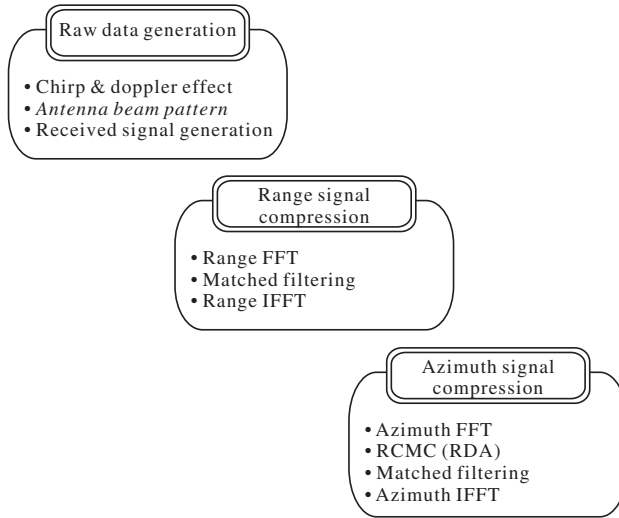
Figure 8. SAR system simulation flow chart.

beamwidth in the azimuth direction due to the identical amplitude distribution. On the other hand, the suggested beam pattern satisfying the mask template has the wide main lobe for matching with a high range resolution. After applying the parameters, the baseband received signal of a point target can be represented as (9) [14].

$$s_r(\tau, \eta) = A_0 w_r\left[\tau - \frac{2R(\eta)}{c}\right] w_a(\eta - \eta_c)\exp\left(-j\frac{4\pi R_0}{\lambda}\right)$$

$$\exp(-j\pi K_a\eta^2)\exp\left\{j\pi K_r\left[\tau - \frac{2R(\eta)}{c}\right]^2\right\} \tag{9}$$

$$w_r(\tau) = rect\left(\frac{\tau}{\tau_{chirp}}\right) \tag{10}$$

$$w_a(\eta) = P_a^2[\theta(\eta)] \tag{11}$$

A_0 is the radar cross section (RCS) of a point target, and w_r represents the duration of the transmit signal as (10). w_a and P_a are the azimuth window function and the azimuth beam pattern in terms of $\theta(\eta)$, respectively. K_a and the K_r express the frequency modulation (FM) in the azimuth direction and the range direction, respectively. After producing the raw data, the range and azimuth compression are performed. We used the range doppler algorithm (RDA), which is one of the most popular methods for the range cell migration correction (RCMC) when azimuth compression was carried out. The point target

simulation of the proposed optimal azimuth beam pattern mode having the parameters listed in Table 3 was performed and compared with the strip-map mode and the spotlight mode to verify the advantages.

Figure 9 shows the results of the strip-map mode simulation, and the azimuth resolution is 0.56 m, which is nearly half of the antenna length. The RCM effect is negligible due to the narrow beamwidth. On the other hand, the azimuth resolution of the spotlight mode simulation
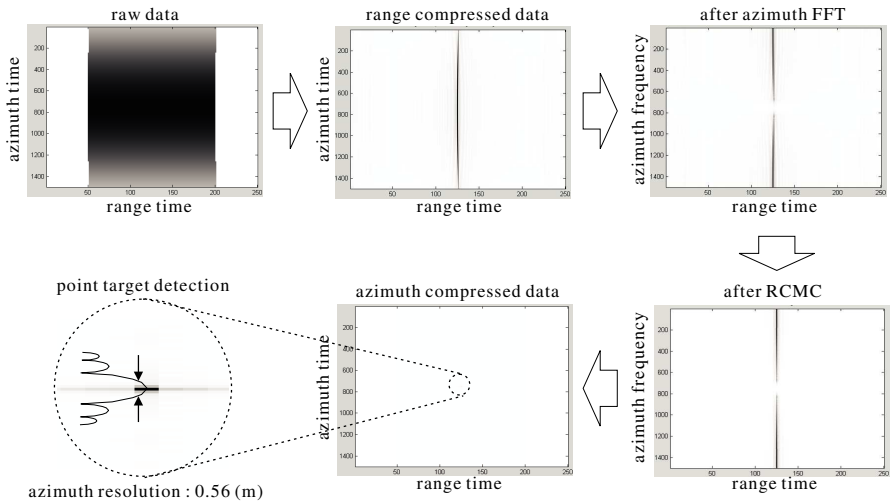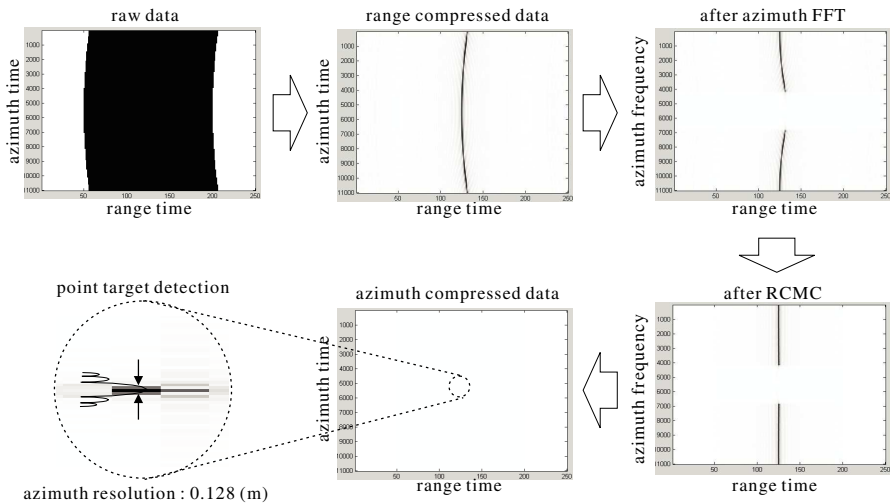

Figure 9. Strip-map mode simulation.

Figure 10. Spotlight mode simulation.

shown in Figure 10 is 0.128 m because the exposure time is increased
by a factor of 4 using beam steering. In this case, the RCMC technique
is needed to correct the migrated image.

Figure 11 shows the result of the proposed optimal azimuth beam
pattern mode simulation. The azimuth resolution of the mode is
increased by the factor of 4 compared with the strip-map mode due
to the four times widen beamwidth. Using the wide main lobe beam
pattern, the obtained image can also be continuous, which is different
from the spotlight mode based on the beam steering.

The performance comparison between the modes are listed in
Table 5 in terms of the target azimuth resolution, antenna azimuth
beamwidth, antenna length, doppler bandwidth, PRF, simulated
azimuth resolution, AAR, and image continuity. The simulated
azimuth resolutions of all modes satisfy the target resolution with few
errors. The beamwidth of the proposed mode is increased by a factor
of 4 compared to the strip-map and spotlight modes to match the high
range resolution, and this results in high azimuth resolution, which is
the same as that of the spotlight mode. All of the modes used the same
antenna length of 1 m. The doppler bandwidth and the PRF of the
spotlight and proposed mode are increased because of the increasing
exposure time. To reduce the AAR, we used the PRF, which has a
bandwidth 1.7 times larger than the doppler bandwidth. The AAR of
the strip-map and the spotlight modes do not meet the requirement
of −20 dB. In contrast, the AAR of the proposed mode is sufficient to
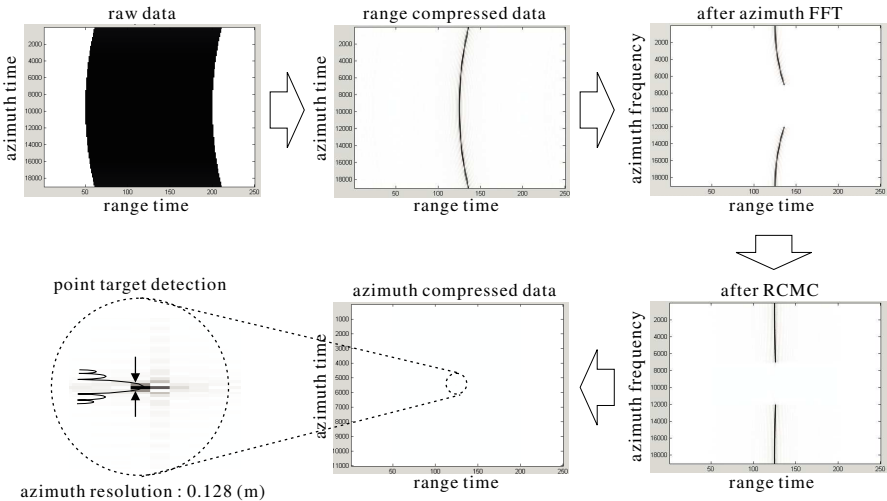meet the condition due to the stairway-shaped side lobe. The image

Figure 11. Proposed optimal azimuth beam pattern mode simulation.

Table 5. Performance comparison between the modes.

	Strip-map	Spotlight	Proposed
Target azimuth resolution	0.5 (m)	0.125 (m)	0.125 (m)
Antenna beamwidth in azimuth	1.64 (deg)	1.64 (deg)	6.63 (deg)
Antenna length	1 (m)	1 (m)	1 (m)
Doppler bandwidth	446 (Hz)	1800 (Hz)	1813 (Hz)
PRF	760 (Hz)	3100 (Hz)	3100 (Hz)
Simulated azimuth resolution	0.56 (m)	0.128 (m)	0.128 (m)
AAR	−10.6 (dB)	−11 (dB)	−21.9 (dB)
Image continuity	o	x	o

continuity can be obtained in all modes except for the spotlight mode. In other words, the proposed mode have the continuous image, which is the advantage of the strip-map mode, and the high resolution image, which is the advantage of the spotlight mode, simultaneously.

5. CONCLUSION

We presented an optimal azimuth beam pattern mask template in terms of the SAR system performances, such as the $NE\sigma_0$, the azimuth resolution, the RA, and the AAR, and suggested an azimuth beam pattern satisfying the mask template using the PSO. The main lobe of the proposed mode is increased by a factor of 4 compared to the strip-map and spotlight modes, and it results in four times the azimuth resolution, which is the same as the resolution of the spotlight mode. Due to the continuous wide beam pattern, the obtained image can also be continuous, which is different from the spotlight mode based on the beam steering. The AAR of the proposed mode is −21.9 dB which is sufficient to meet the requirement of −20 dB due to the stairway-shaped side lobe. The suggested mode, therefore, guarantees continuous and high resolution images simultaneously with low AAR.

REFERENCES

1. Curlander, J. C. and R. N. McDonough, *Synthetic Aperture Radar Systems and Signal Processing*, John Wiley and Sons, Inc., 1991.

2. Chan, Y. K. and V. C. Koo, "An introduction to synthetic aperture radar (SAR)," *Progress In Electromagnetics Research B*, Vol. 2, 27–60, 2008.

3. Chan, Y. K. and S. Y. Lim, "Synthetic aperture radar (SAR) signal generation," *Progress In Electromagneitcs Research B*, Vol. 1, 269–290, 2008.

4. Li, W. T., X. W. Shi, L. Xu, and Y. Q. Hei, "Improved GA and PSO culled hybrid algorithm for antenna array pattern synthesis," *Progress In Electromagnetics Research*, Vol. 80, 461–476, 2008.

5. Li, J. F., B. H. Sun, Q.-Z. Liu, and L. Gong, "PSO-based fast optimization algorithm for broadband array antenna by using the cubic spline interpolation," *Progress In Electromagneitcs Research Letters*, Vol. 4, 173–181, 2008.

6. Lim, T. S., V. C. Koo, H. T. Ewe, and H. T. Chuah, "A SAR autofocus algorithm based on particle swarm optimization," *Progress In Electromagnetics Research B*, Vol. 1, 159–176, 2008.

7. Gies, D. and Y. Rahmat-Samii, "Particle swarm optimization for reconfigurable phase-differentiated array design," *Microwave Opt. Technol. Lett.*, Vol. 38, No. 3, 168–175, 2003.

8. Robinson, J. and Y. Rahmat-Samii, "Particle swarm optimization in electromagnetics," *IEEE Trans. Antennas Propagat.*, Vol. 52, No. 2, 397–407, 2004.

9. Boeringer, D. W. and D. H. Werner, "Particle swarm optimization versus genetic algorithms for phased array synthesis," *IEEE Trans. Antennas Propagat.*, Vol. 52, No. 3, 771–779, 2004.

10. Kim, S. Y., N. H. Myung, and M. J. Kang, "Antenna mask design for SAR performance optimization," *IEEE Geosci. Remote Sens. Lett.*, Vol. 6, No. 3, 443–447, 2009.

11. Kim, S. Y. and N. H. Myung, "An optimal antenna pattern synthesis for active phased array SAR based on particle swarm optimization and adaptive weighting factor," *Progress In Electromagnetics Research C*, Vol. 10, 129–142, 2009.

12. Islam, M. T., M. Moniruzzaman, N. Misran, and M. N. Shakib, "Curve fitting based particle swarm optimization for uwb patch antenna," *Journal of Electromagnetic Waves and Applications*, Vol. 23, No. 17–18, 2421–2432, 2009.

13. Zhang, L., F. Yang, and A. Z. Elsherbeni, "On the use of random variables in particle swarm optimizations: A comparative study of gaussian and uniform distributions," *Journal of Electromagnetic Waves and Applications*, Vol. 23, No. 5–6, 711–721, 2009.

14. Cumming, I. G. and F. H. Wong, *Digital Processing of Synthetic Aperture Radar*, Artech House, 2005.